

Table 1. Absolute (hartree)^a and relative (kJ mol⁻¹) energies of the systems involved in the description of protonation of trimethyl phosphite

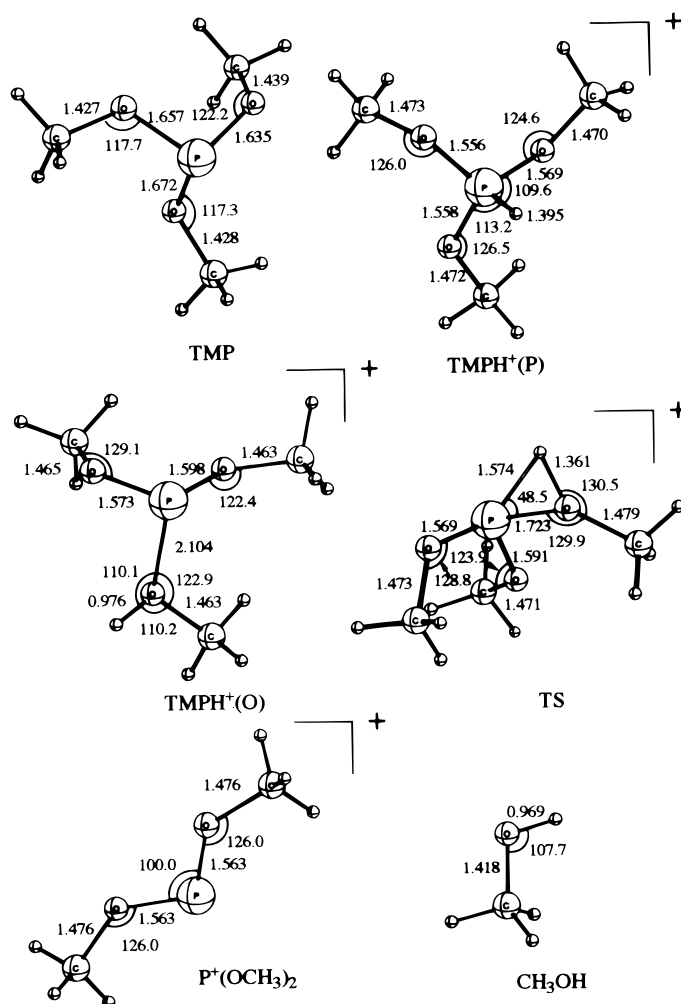
Species	B3LYP 6-31G(d)	ZPE 6-31G(d)	E REL (ZPC) 6-31G(d)	B3LYP 6-311+G(2df,p)	E REL (ZPC) 6-311+G(2df,p)
TMP	-686.779 332	0.129 278	911	-686.955 233	917
TMPH ⁺ (P) ^b	-687.138 327	0.141 105	0.0	-687.316 258	0.0
TMPH ⁺ (O) ^c	-687.113 208	0.140 854	65	-687.285 315	80
TS ^d	-687.032 171	0.135 304	264	-687.208 140	269
P ⁺ (OCH ₃) ₂	-571.354 392	0.086 202	—	-571.479 655	—
CH ₃ OH	-115.714 404	0.051 459	—	-115.769 623	—
P ⁺ (OCH ₃) ₂ + CH ₃ OH	-687.068 796	0.137 661	174	-687.249 278	167

^a 1 hartree = 2625.5 kJ mol⁻¹.^b TMP protonated on the phosphorus atom.^c TMP protonated on an oxygen atom.^d Transition state between the two protonated forms.

with neutral TMP but also to form an adduct with water (water is always present at trace levels in the QIT). In addition, this adduct protonates neutral TMP. In order to understand the formation and the reactivity of protonated TMP, we also report the results of high-level *ab initio* calculations.

EXPERIMENTAL

All experiments were carried out with a QIT (Saturn 3; Varian, Walnut Creek, CA, USA) coupled with a Varian Star 3400 CX gas chromatograph. A 30 m × 0.25

**Figure 1.** Equilibrium geometries of neutral, protonated and fragment isomers for TMP, optimized at the B3LYP/6-31G(d) level. Bond lengths are in Å and angles in degrees.

mm i.d. DB 5 fused-silica capillary column with a 0.25 μm film thickness was used for all analyses. The helium flow was adjusted to give a column head pressure of 10 psi (1 psi = 6.895 kPa). The transfer line temperature from the gas chromatograph to the QIT was held at 260 °C and the QIT manifold temperature was 170 °C. The TMP was obtained from Fluka and diluted in pentane to a concentration of 100 ppm.

The ion–molecule reactions were carried out under the following conditions: 1 μl of the above TMP solution was injected into the chromatograph in the splitless mode with the injector held at 185 °C. The GC column was held at 50 °C for 5 min and then ramped to 100 °C at 10 °C min^{-1} and held at that temperature for 5 min. The QIT was operated using the Varian version 5.0 software. The data acquisition sequence was composed of (1) 70 eV electron impact of TMP, (2) isolation of the $\text{O}=\text{P}(\text{OCH}_3)_2^+$ ion (m/z 109) with a mass isolation windows of 3 m/z (ions of masses 108, 109 and 110 are isolated) and adjustments of the amplitude of the 1.05 MHz r.f. voltage applied to the ring electrode so as to store ions of m/z 109 at a selected value of the Mathieu parameter q_z (~ 0.4), (3) reaction time up to 125 ms with neutral TMP, as it eluted from the GC column, and (4) ejection and detection (tandem mass spectra) of product ions using the mass-selective instability scan⁷ with dipolar resonance ejection at a fixed frequency of 0.485 MHz.⁸ In CID experiments, the stored ion of interest was resonantly excited⁹ by the application of a supplementary a.c. voltage to the end-cap electrode at an appropriate voltage. A prototype software ('Toolkit') was used for MS⁵ experiments. Protonation of TMP was carried out with methane and anhydrous ammonia. In each case, the reagent gas pressure in the ion trap was $\sim 10^{-5}$ – 2×10^{-5} Torr (1 Torr = 133.3 Pa).

CALCULATIONS

The geometries of the considered protonated isomers of TMP have been fully optimized using the DFT approach with non-local corrections (B3LYP), using a split valence basis set including polarization functions in heavy atoms, 6–31G(d).¹⁰ This corresponds to a so-called hybrid method, which includes a mixture of Hartree–Fock, Slater and Becke exchange functionals. Here we used the Becke three-parameter non-local exchange functional,¹¹ combined with the non-local correlation functional of Lee, Yang and Parr (LYP).¹² This method has recently been shown to be reliable in the prediction of energetics and geometries for a wide variety of systems.¹³ Vibrational frequencies have been obtained at the same level of theory for the stationary points on the hypersurface, in order to characterize the nature of these points with the number of imaginary frequencies: all frequencies being real indicates a minimum, and one imaginary frequency is characteristic of a transition state. The evaluation of the vibrational frequencies allows us also to correct for zero point energies (ZPE). The same level of theory is applied for methanol, $\text{:P}(\text{OCH}_3)_2^+$ and neutral TMP in order to evaluate energy differences coherently. From the transition state geometry we performed intrinsic reaction

coordinate (IRC)¹⁴ calculations in order to confirm the reactants and products to which this TS leads. In order to compensate for possible shortcomings of the relatively small basis set 6–31G(d), we performed single-point calculations on both protonated forms and fragments at the triply split valence 6–311 + G(2df,p) basis set,¹⁵ which includes polarization functions at hydrogen atoms and diffuse functions on the heavy atoms. All the calculations were performed using the Gaussian-94¹⁶ series of programs. The calculated total energies and the relative energies are reported in Table 1. The optimized structures are shown in Fig. 1.

RESULTS AND DISCUSSION

The isolated phosphonium ions $\text{OP}(\text{OCH}_3)_2^+$ (m/z 109) were allowed to react with neutral TMP for 60 ms. The resulting ion–molecule reaction products were identified by MS/MS (Fig. 2). The spectrum contains four species in addition to the m/z 109 ion: m/z 93, 125, 127 and 155, which are the result of various different reaction paths.

The ions of m/z 93 and m/z 155 come from reactions between m/z 109 and neutral TMP as shown previously,⁶ but the abundance ratios of these two ions are different: 100:1 in the ICR cell and 4:1 in the QIT. For the same reaction time the $\text{O}=\text{P}(\text{OCH}_3)_2^+$ reactant ion is nearly entirely consumed in the ICR cell. In making such a comparison it must be noted that the conditions in the QIT and those in a ICR cell are not identical. The QIT is typically operated at pressures higher than those of an ICR cell. It is generally accepted that the ions in a QIT are cooled kinetically by collisions with the buffer gas.¹⁷ One possible channel for kinetic cooling is conversion into internal energy. These factors can cause differences in ion–molecule product distributions.

The two other product ions at m/z 127 and 125 cannot be formed by ion–molecule reactions between m/z 109 and neutral TMP. In fact, the ion at m/z 127 is the result of addition of the background water to the m/z 109 ion. Such reactions have been reported recently for the m/z 109 ion¹⁸ and various phosphonate product ions.¹⁹ The structure of the m/z 127 ion corresponds to protonated dimethyl phosphate, $[(\text{CH}_3\text{O})_2\text{P}(\text{OH})_2]^+$.

The m/z 125 ion appears to correspond to protonated trimethyl phosphite. If we consider that the proton affinities (PA) of dimethyl phosphate and trimethyl phosphate should be similar (887 kJ mol^{-1}),²⁰ the stronger base TMP ($PA = 923 \text{ kJ mol}^{-1}$)²⁰ ought to be able to deprotonate the protonated dimethyl phosphate. To obtain confirmation of this proton transfer between m/z 127 and neutral TMP, a triple mass spectrum was recorded. The spectrum shows that the isolated m/z 127 ion generated from the mass-selected m/z 109 ion reacts with neutral TMP to give only one ion–molecule reaction product at m/z 125. Note that the formation of an ion at m/z 93 by loss of methanol from protonated TMP is not observed under our experimental conditions. This point, which conflicts with the results of Zeller *et al.*⁵ (Scheme 1), will be discussed below.

In summary, the m/z 109 ion can react with neutral trimethyl phosphite according to two methoxy transfers: one from m/z 109 to TMP to give m/z 93 and the

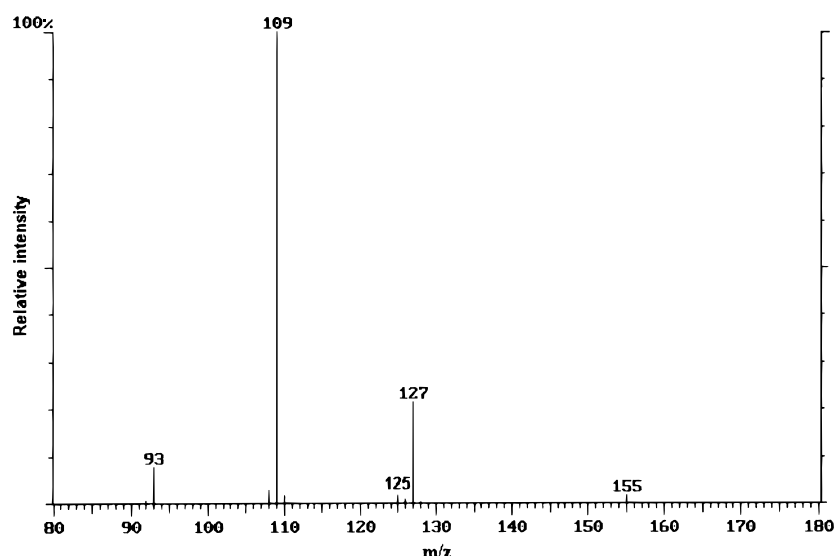
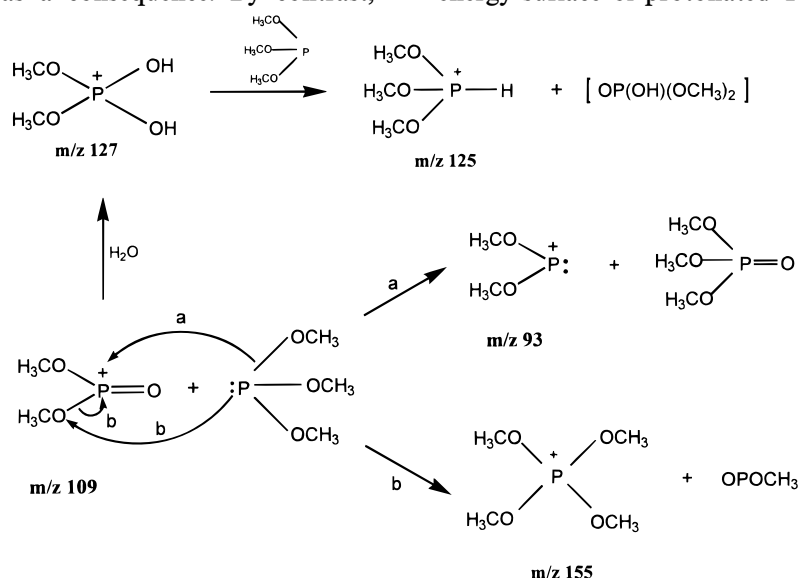


Figure 2. Tandem mass spectrum of the m/z 109 ion, isolated during 60 ms without the application of supplemental excitation potential.

other from TMP to m/z 109 to yield m/z 155. In addition, the ion at m/z 109 reacts with residual water present in the QIT to give an adduct at m/z 127, which subsequently protonates the neutral TMP. These different processes are summarized in Scheme 2.

In order to clarify the loss of a molecule of methanol from protonated TMP, *ab initio* calculations and supplementary experiments were undertaken. The elimination of methanol from protonated TMP can be the result of two processes, which depend of the site of protonation: (i) a direct protonation on an oxygen atom or (ii) a protonation (as in solution²¹) on the phosphorus followed by a 1,2-proton shift. Except for the experimental *PA* of TMP,²⁰ no other thermochemical data are available, to the best of our knowledge. Hence we considered it of interest to carry out a study using high-level *ab initio* calculations, which should provide useful information to explain the unimolecular chemistry of protonated TMP. Geometrically, one can observe by inspection of Fig. 1 that when protonation takes place at the more electronegative O atom, the P—O bond weakens as a consequence. By contrast,

protonation at phosphorus is accompanied by a strengthening of the P—O linkage. This general behaviour has been reported²² in similar circumstances and can be explained as follows: when the charged H^+ approaches the more electronegative atom, the oxygen donates charge to the proton, and this charge is mainly taken from the P—O linkage. On the other hand, when H^+ approaches the less electronegative phosphorus atom, the higher electronegativity of O opposes the depopulation of the P—O linkage, and the phosphorus atom can only polarize the bond, reinforcing it and consequently making the P—O distance shorter. This effect is, in this particular case, very strong: the *O*-protonated isomer has a P—O distance which is elongated by about 0.5 Å and can be viewed as a methanol- $P(OCH_3)_2^+$ complex, where Mulliken population analysis locates the charge mainly on phosphorus. Both the long P—O distance and the concentration of charge at P lead to the supposition that there is no barrier for the elimination of a methanol molecule. We present in Fig. 3 the potential energy surface of protonated TMP, which corresponds



Scheme 2

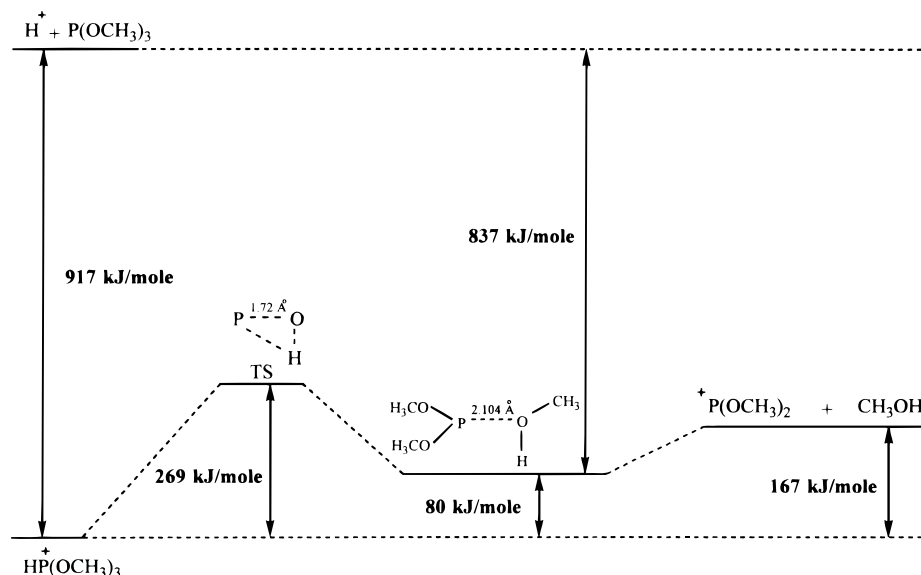


Figure 3. Potential energy surface of protonated TMP.

to the protonation of TMP on phosphorus, on oxygen, the transition state between two protonated forms and the final state for the methanol elimination.

The calculated ΔH for protonation on phosphorus at our highest level of calculation is 917 kJ mol^{-1} , showing excellent agreement with experiment ($PA = 923 \text{ kJ mol}^{-1}$),²⁰ and justifies our choice of the DFT method. The *O*-protonated species is predicted to be 80 kJ mol^{-1} less stable than the *P*-protonated form. Assuming that there is no barrier for protonation, this is expected to be favoured at the P atom. The barrier for conversion to the *O*-protonated isomer was found to be 269 kJ mol^{-1} and identified by means of IRC calculations to connect both protonated forms. This substantial barrier ensures the presence of both isomers, depending on the conditions of the experiment, with thermodynamics favouring the *P*-protonated form. Under higher energy conditions, the barrier can be traversed and an easy subsequent loss of methanol can be expected.

These *ab initio* calculations are in good agreement with our experimental results and those of Hodges *et al.*⁶ The ion at m/z 127, protonated dimethyl phosphate ($PA \approx 887 \text{ kJ mol}^{-1}$), cannot protonate TMP on oxygen since the reaction would be endothermic by $\sim 50 \text{ kJ mol}^{-1}$. When protonation occurs on phosphorus, the unimolecular isomerization between *P*- and *O*-protonated forms is thermodynamically impossible. The exothermic protonation on the phosphorus atom provides only $\sim 30 \text{ kJ mol}^{-1}$, which is far below the energy barrier for the isomerization (Table 1 and Fig. 3). One can therefore conclude that the observed m/z 93 ion (Fig. 2) comes only from the ion-molecule reaction between the ion at m/z 109 and neutral TMP. To confirm this assumption, two other CI experiments were undertaken. As shown in Table 2, when methane is used to protonate TMP, formation of an ion at m/z 93 by loss of methanol from protonated TMP is a very efficient process.

In contrast, when protonation is carried out with ammonia, the abundance of the m/z 93 ion falls drastically (Table 2). These results can be easily explained on

the basis of energetic considerations. Methane ($PA = 551 \text{ kJ mol}^{-1}$)²⁰ can protonate TMP either on an oxygen atom ($PA = 837 \text{ kJ mol}^{-1}$) or on phosphorus ($PA = 923 \text{ kJ mol}^{-1}$). Moreover, the exothermicity of the reaction ($\sim 372 \text{ kJ mol}^{-1}$) could provide enough energy to overcome the activation barrier (269 kJ mol^{-1}) corresponding to the proton migration between phosphorus and an oxygen. In other words, whatever the site of protonation, when methane is used as a CI gas reagent, the formation of the m/z 93 ion by loss of methanol from protonated TMP is thermodynamically possible. Note that the CI spectrum of TMP (Table 2) with methane displays two ions at higher mass than m/z 125, namely m/z 153 and 165, which are the results of adducts between neutral TMP and C_2H_5^+ and C_3H_5^+ , respectively (two ions that are present in the CH_4 plasma). When the protonation of TMP is performed with NH_3 ($PA = 854 \text{ kJ mol}^{-1}$),²⁰ protonation on oxygen is slightly endothermic ($\sim 17 \text{ kJ mol}^{-1}$) and the elimination of methanol becomes a minor process. In summary, the unimolecular reactivity of protonated TMP prepared using three different reagents, dimethyl phosphate, CH_4 and NH_3 , is in accordance with theoretical data.

The only point that remains unclear from a thermodynamic point of view is the elimination of methanol from protonated TMP that is formed by proton transfer from protonated trimethyl phosphate, as observed by Zeller *et al.*⁵ In fact, an explanation of this result may arise from the method of preparation used by these authors for the formation of protonated trimethyl phosphate. Those ions were generated by self-chemical ionization, wherein fragment ions obtained by electron ionization-induced dissociation are used to protonate

Table 2. Chemical ionization mass spectrum of trimethyl phosphite (product ion m/z with relative abundance (%) in parentheses)

$\text{Cl}(\text{CH}_4)$	93 (100)	125 (27)	153 (11)	165 (2)
$\text{Cl}(\text{NH}_3)$	93 (5)	125 (100)		

the neutral trimethyl phosphate. The $(\text{CH}_3\text{O})_2\text{POH}^+$, $\text{CH}_3\text{OP}(\text{OH})=\text{O}^+$, $\text{CH}_3\text{OP}(\text{H})\text{OH}^{++}$ and CH_3OPOH^+ fragment ions can reasonably protonate the trimethyl phosphate at two different oxygens, the methoxy and the $\text{P}=\text{O}$ group. Hence the ion–molecule reactions between protonated trimethyl phosphate (a mixture of protonated forms) and neutral TMP could produce both protonated forms of TMP. Subsequently *O*-protonated TMP could spontaneously eliminate without activation barrier a molecule of methanol. The m/z 125:93 branching ratio, reported as 8.5:1.5, suggests that the *P*-protonated form is predominant.

CONCLUSION

Gas-phase ion–molecule reactions of the phosphonium ion $\text{OP}(\text{OCH}_3)_2^+$ with neutral TMP were carried out on a QIT mass spectrometer. The formation of primary

products of m/z 93 and 155 agree with results obtained in a previous ICR study.⁶

Nevertheless, the reaction conditions differ sufficiently to produce other reaction products, namely protonated dimethyl phosphate (which is formed by the addition of a water molecule), and protonated TMP (which is the result of proton transfer between protonated dimethyl phosphate and TMP as shown by MS^3 experiments). High-level *ab initio* calculations and CI ionization experiments clarify the loss of methanol from protonated TMP and demonstrate that the proportions of the *P*- and *O*-protonated forms depend on the reagent gas.

Acknowledgements

We thank Dr J. Tortajada for helpful discussions. A. Luna gratefully acknowledges a postdoctoral TMR grant from the European Community.

REFERENCES

1. J. C. Occolowitz and G. L. White, *Anal. Chem.* **35**, 1179 (1963).
2. J. R. Holtzclaw, J. R. Wyatt and J. E. Campana, *Org. Mass Spectrom.* **20**, 90 (1985).
3. A. P. Snyder and C. S. Harden, *Org. Mass Spectrom.* **25**, 53 (1990).
4. L. C. Zeller, J. T. Farrell, Jr, H. I. Kenttämää and T. Kirivalanen, *J. Am. Soc. Mass Spectrom.* **4**, 124 (1992).
5. L. Zeller, J. Farrell, Jr, P. Vainiotalo and H. I. Kenttämää, *J. Am. Chem. Soc.* **114**, 1205 (1992).
6. R. V. Hodges, T. J. McDonnell and J. L. Beauchamp, *J. Am. Chem. Soc.* **102**, 1327 (1980).
7. G. C. Stafford, Jr, P. E. Kelley, J. E. P. Syka, W. E. Reynolds and J. F. J. Todd, *Int. J. Mass Spectrom. Ion Processes* **60**, 85 (1984).
8. D. B. Tucker, C. H. Hameister, S. C. Bradshaw, D. J. Hoekam and M. Weber-Graban, in *Proceedings of the 36th Conference on Mass Spectrometry and Allied Topics*, San Francisco, CA, 1988, pp. 620–629.
9. B. Bolton, G. Wells and M. Wang, in *Proceedings of the 41st Conference on Mass Spectrometry and Allied Topics*, San Francisco, CA, 1993, p. 474.
10. R. Ditchfield, W. J. Hehre and J. A. Pople, *J. Chem. Phys.* **54**, 724 (1971); W. J. Hehre, R. Ditchfield and J. A. Pople, *J. Chem. Phys.* **56**, 2257 (1972); P. C. Hariharan and J. A. Pople, *Theor. Chim. Acta* **28**, 213 (1973); *Mol. Phys.* **27**, 209 (1974); M. S. Gordon, *Chem. Phys. Lett.* **76**, 163 (1980).
11. A. D. Becke, *J. Chem. Phys.* **96**, 2155 (1992); **98**, 5648 (1993).
12. C. Lee, W. Yang and R. G. Parr, *Phys. Rev. B* **37**, 785 (1988).
13. A. Ricca and C. W. Bauschlicher, *J. Phys. Chem.* **98**, 12899 (1994); **99**, 5992, (1995), **99**, 9003 (1995) and references cited therein; Q. Cui, D. G. Musaev, M. Svensson, S. Sieber and K. Morokuma, *J. Am. Chem. Soc.* **117**, 12366 (1995); A. Luna, A. M. Mebel and K. Morokuma, *J. Chem. Phys.* **105**, 3187 (1996); A. I. González, O. Mó, M. Yáñez, E. León, J. Tortajada, J. P. Morizur, I. Leito, P. C. Maria and J. F. Gal, *J. Phys. Chem.* **100**, 10490 (1996).
14. C. González and H. B. Schlegel, *J. Phys. Chem.* **90**, 2154 (1989).
15. R. Krishnan, J. S. Binkley, R. Seeger and J. A. Pople, *J. Chem. Phys.* **72**, 650 (1980); A. D. McLean and G. S. Chandler, *J. Chem. Phys.* **72**, 5639 (1980).
16. M. J. Frisch, G. W. Trucks, H. B. Schlegel, P. M. W. Gill, B. G. Johnson, M. A. Robb, J. R. Cheeseman, T. Keith, G. A. Peterson, J. A. Montgomery, K. Raghavachari, M. A. Al-Laham, V. G. Zakrzewsky, J. V. Ortiz, J. B. Foresman, J. Cioslowski, B. B. Stefanov, A. Nanayakkara, M. Challacombe, C. Y. Peng, P. Y. Ayala, W. Chen, M. W. Wong, J. L. Andres, E. S. Replogle, R. Gomperts, R. L. Martin, D. J. Fox, J. S. Binkley, D. J. Defrees, J. Baker, J. J. P. Stewart, M. Head-Gordon, C. Gonzalez and J. A. Pople, *Gaussian 94, Revision D.1*. Gaussian, Inc., Pittsburgh, PA, 1995.
17. M. J. Charles and G. L. Glish, in *Practical Aspects of Ion Trap Mass Spectrometry*, edited by R. E. March and J. F. J. Todd, Vol. III, p. 89. CRC Press, Boca Raton, FL (1995).
18. J. P. Morizur, M.-H. Taphanel, S. Gevrey, M. L. Bouguerra and M. R. Driss, *Analysis* **24**, 177 (1996).
19. M. W. Wensing, B. E. Farch, R. A. Fifer, A. P. Snyder and C. S. Harden, in *Proceedings of the 43rd Conference on Mass Spectrometry and Allied Topics*, Atlanta, GA, 1995, p. 373.
20. S. G. Lias, J. E. Bartness, J. F. Liebman, J. L. Holmes, R. D. Levin and W. G. Mallard, *J. Phys. Chem. Ref. Data* **17**, Suppl. (1988).
21. G. A. Olah and C. W. McFarland, *J. Org. Chem.* **36**, 1374 (1971).
22. M. Alcamí, O. Mó, M. Yáñez, J. L. Abboud and J. Elguero, *Chem. Phys. Lett.* **172**, 471 (1990).